limit only: M_a is calculated according to eq 11 (in our case, see column 6 of Table II). On the contrary, if one knows M_s, the uncertainty limits are in between M_s and M_a (columns 5 and 6). Table II also shows the limit values M_a and M_{ph} of the molecular weight corresponding to the experimental $|f^*|$ that should be considered in the case (columns 6 and 7) when M_s is not known but ϕ could be evaluated. The values of column 7 in parentheses refer to points that are below the theoretical line b. These points are characterized by $\phi < \phi_s$ due to synthesis imperfections, and therefore the corresponding M_{ph} values must not be considered.

As a final remark we observe that tensile tests of swollen networks have the advantage, compared to those of dry materials, of allowing the equilibrium to be reached more quickly, which makes the experimental work easier. Moreover, they allow one to examine also some glassy polymers when their T_g's in the swollen state become lower than room temperature, at which tensile tests are performed. All the above considerations can be extended to dry networks by putting $v_2 = 1$.

Acknowledgment. We thank F. Bianchi and P. Donzelli for their help in performing mechanical tests. The Progetto Finalizzato Chimica Fine e Secondaria CNR and ENIRICERCHE Co. are also gratefully acknowledged for their financial support.

References and Notes

(1) Flory, P. J. In *Principles of Polymer Chemistry*; Cornell University Press: Ithaca, NY, 1953.
(2) James, H. M.; Guth, E. *J. Chem. Phys.* **1953**, *21*, 1039.
(3) Treloar, L. R. G. In *The Physics of Rubber Elasticity*, 2nd ed.; Clarendon Press: Oxford, 1958.
(4) Flory, P. J. *J. Chem. Phys.* **1977**, *66*, 5720.
(5) Flory, P. J. *Polymer* **1979**, *20*, 1317.
(6) Flory, P. J. *Macromolecules* **1979**, *12*, 119.
(7) Erman, B.; Flory, P. J. *Macromolecules* **1982**, *15*, 800.
(8) Pegoraro, M.; Penati, A.; Zanderighi, L. XVIII FATIPEC Congress, Italy, Venice, 1986; Vol. 3, p 203.
(9) David, D. J.; Staley, H. B. In *Analytical Chemistry of the Polyurethanes*; Wiley: New York, 1969; Part 3, p 289.
(10) Flory, P. J. *J. Am. Chem. Soc.* **1936**, *58*, 1877.
(11) Esposito, P.; Pagliarani, L. Thesis, Polytechnic of Milan, Italy, 1982-1983.
(12) Zamboni, V.; Flisi, U.; Giunchi, G. *Rubber Chem. Technol.* **1971**, *44*, 1109.
(13) Minutillo, A. Thesis, Specialization School in Polymer Science, Polytechnic of Milan, Italy, 1986-1987.

Viscoelastic Properties of Telechelic Ionomers. 2. Complexed α,ω-Diamino Polydienes

Pascal Charlier, Robert Jérôme,* and Philippe Teyssié

Laboratory of Macromolecular Chemistry and Organic Catalysis, University of Liège, Sart-Tilman, B6, 4000 Liège, Belgium

L. A. Utracki

National Research Council of Canada, Industrial Materials Research Institute, Boucherville, Quebec, Canada, J4B 6Y4

Received October 25, 1989; Revised Manuscript Received January 29, 1990

ABSTRACT: Complexation of the end groups of amino telechelic polydienes strongly affects the viscoelastic behavior. This is shown in the thermal dependence of the isochronous torsion modulus of a liquid polybutadiene selectively end-capped by a piperazine unit at both extremities. A rubbery plateau emerges when the telechelic polymer is coordinated to copper(II) or iron(III) chlorides. The rubbery plateau extends over a temperature range that depends on the molar ratio of the transition metal to the amine end group. Similar observations have been reported when the dynamic mechanical properties of an α,ω-bis(dimethylamino) telechelic polyisoprene have been investigated over the full range of temperature from the glassy plateau to the viscous flow. Upon complexation of the end groups, a rubberlike plateau is observed, which does not exist for the uncomplexed polymer. Furthermore, a secondary relaxation, attributed to the aggregation of the complexed amine end groups, occurs above T_g. The temperature at which the maximum of this relaxation is observed and the distribution of the relaxation times depend on the metal to amine end-group molar ratio. At a ratio of 1, $FeCl_3$ endows the chain network with higher cross-link density than $CuCl_2$ does. However, at the same time the temperature width of the rubbery plateau is much shorter for the former than for the latter polymer, indicating a relative thermal instability of the Fe-amine complexes.

Introduction

Thermomechanical properties of hydrophobic polymers are known to be modified by ionic groups randomly distributed along a polymeric backbone.[1,2] Interest in ionomers has to be found in the potential of cross-linking macromolecules in a thermoreversible manner. Alternative modifications of traditional polymers consist in replacing the ionic groups by other types of interacting groups. Examples have been described in which ligands have been attached onto polymeric chains and engaged in coordination reactions with metal salts.[3-5] Although many ligands can be used, this work focalizes on amino groups, which are one of the most studied groups both in solution and in solid state.[3-6] As recent papers indicate, there is plenty of interest in these systems.[7-15]

The ability of ligands to form complexes with transition-metal salts is responsible for a transient network formation. Although the coordinated salts may act as mutually interacting dipoles, the coordination number of the transition-metal ion is expected to promote temporary cross-links.[16]

This paper deals with the possible improvement of the mechanical properties of a nonpolar polymer that the complexation of the amino end groups with a transition-metal salt can promote. As previously reported, telechelic polymers have been designed as models for the more complex systems in which the functional groups are randomly attached to the chain.[2] This approach has been fruitful in understanding the ion pair association and its effect on the macroscopic properties of ionomers.[17-21] Now the concept is extended to dimethylamino telechelic polydienes in order to examine the effect of the coordination of the end groups on the formation of a transient network and the breadth of the rubbery plateau zone. For the sake of comparison, the dynamic mechanical properties of the same α,ω-bis(dimethylamino)polyisoprene quaternized with several alkyl iodides have been studied and reported elsewhere.[21] The present paper may be considered as an extension of that study. Now the following questions are addressed: how does the coordinative association of the end groups compare with the electrostatic interactions of quaternary ammonium pairs and to what extent does the transition metal to the amine end-group molar ratio affect the mechanical properties of the polymer? Besides the α,ω-bis(dimethylamino)-polyisoprene, a sample of polybutadiene end-capped with a piperazine unit has also been studied.

Experimental Section

α,ω-Dipiperazinopolybutadiene (PBD). α,ω-Dipiperazinopolybutadiene was supplied by BFGoodrich under the trade name "Hycar ATB". The main molecular features were $\bar{M}_n$ = 4000 (vapor pressure osmometry), $\bar{M}_w/\bar{M}_n$ = 1.8 (size-exclusion chromatography), average functionality = 2 piperazines/chain (according to the manufacturer), and cis/trans/vinyl ratio = 20/65/15 (NMR). The structure of the piperazine end group was

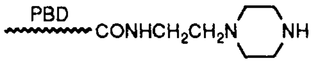

Thus, each end group consisted of one tertiary and one secondary amine function. This telechelic polybutadiene will be designated as "PBD(pip)$_2$".

α,ω-Bis(dimethylamino)polyisoprene (PIP). The anionic polymerization of isoprene was performed in a previously flamed and nitrogen-purged glass reactor equipped with rubber septums. Hypodermic syringes and stainless steel capillaries were used to handle liquid products under a nitrogen atmosphere.

Tetrahydrofuran (THF) (pure grade) was dried by refluxing over benzophenone–sodium and distilled under a nitrogen atmosphere. Isoprene (pure grade) was dried over calcium hydride at room temperature and distilled under reduced pressure. It was finally mixed with *n*-BuLi and distilled just before polymerization. 1-Chloro-3-(dimethylamino)propane (DMAPC) resulted from the neutralization of DMAPC·HCl by sodium hydroxide in water. DMAPC was recovered by repeated extractions with diethyl ether. It was dried over anhydrous sodium sulfate and calcium hydride, respectively, for at least 3 days; it was finally distilled just before use.

α,ω-Bis(dimethylamino)polyisoprene was anionically prepared in THF at −78 °C. Sodium–naphthalene was used as a difunctional initiator. It was prepared by reacting naphthalene with an excess of sodium in anhydrous THF. The living macrodianion was deactivated by anhydrous DMAPC and precipitated in methanol. The α,ω-bis(dimethylamino)polyisoprene was purified by three precipitations from THF in methanol.

Table I
Composition of α,ω-Diamino Polydienes Complexed with a Transition-Metal Chloride M_TCl_x

PBD(pip)$_2$-4000			PIP(NMe$_2$)$_2$-5000		
	M_TCl_x, mol %	M_TCl_x, wt %		M_TCl_x, mol %	M_TCl_x, wt %
PBD–Cu-0.5	1.31	3.15	PIP–Cu-0.50	1.27	2.46
PBD–Cu-1	2.63	6.3	PIP–Cu-0.75	1.91	3.69
PBD–Cu-2	5.26	12.6	PIP–Cu-0.10	2.55	4.92
PBD–Cu-3	7.89	18.9	PIP–Cu–1.25	3.19	6.15
			PIP–Cu-1.50	3.82	7.38
PBD–Fe-0.5	1.31	3.75	PIP–Fe-1.0	2.55	5.87
PBD–Fe-1	2.63	7.5			
PBD–Fe-2	5.26	15			
PBD–Fe-3	7.89	22.5			

The PIP microstructure was characterized by a 3,4/1,2 ratio of 65/35. Molecular weight was controlled by the monomer/catalyst molar ratio. It was determined by vapor pressure osmometry ($\bar{M}_n$ = 5200). Polydispersity was calculated as $\bar{M}_w/\bar{M}_n$ = 1.3 by size-exclusion chromatography. The functionality was determined by potentiometric titration of the dimethylamino end groups using perchloric acid (0.02 mol/L) in a 9/1 toluene/methanol mixture. From the titration result and the $\bar{M}_n$ value, polyisoprene was found to be end-capped by 1.9 amino groups.

Complexation of the Amino Groups. Both PBD(pip)$_2$ and PIP(NR$_2$)$_2$ were dissolved in toluene (5%), and the resulting solution was added dropwise with a solution of $CuCl_2 \cdot 2H_2O$ or $FeCl_3 \cdot 6H_2O$ in methanol (0.2 mol/L) under vigorous stirring at 25 °C for at least 24 h. No precipitation occurred, and the solution remained homogeneous through the whole process. The complexed polymers were recovered by solvent distillation under vacuum at room temperature. They were dried to constant weight at 60–70 °C for at least 1 mo. An amount of 1 wt % of antioxidant (Irganox 1010) was added to solutions of PBD(pip)$_2$ and PIP(NR$_2$)$_2$ prior to complex formation.

The Cu^{2+} (and Fe^{3+}) to piperazine group molar ratio was x = 0.5, 1.0, 2.0, and 3.0, respectively. The Cu^{2+} to dimethylamine group ratio was 0.5, 0.75, 1.0, 1.25, and 1.5, respectively. Only one PIP sample with a Fe/dimethylamine ratio of 1.0 was prepared. Table I provides the composition of all the samples bearing amino end groups complexed with a transition-metal salt (M_TCl_x).

Differential Scanning Calorimetry (DSC). The DSC thermograms were recorded from 243 to 393 K and from 143 to 273 K for the PIP and the PBD samples, respectively. A Perkin-Elmer DSC-4 was used at a heating rate of 20 °C/min with a constant flow of dry nitrogen over the sample.

Torsion Pendulum. Specimens (2 × 8 × 40 mm) were compression molded at 393 K and 2 MPa for 15 min. They were used in a (static) Gehman torsion pendulum instrument to record isochronous (10 s) moduli from 173 to 393 K.

Dynamic Mechanical Measurements. A dynamic mechanical thermal analyzer (DMTA from Polymer Laboratories) was used in the temperature range below the glass transition temperature, T_g. At higher temperatures, $T > T_g$, a Rheometrics mechanical spectrometer (RMS 605 S) was used with a parallel-plate geometry. The 25-mm-diameter specimens in a 1.4-mm-wide gap were tested under a constant flow of dry nitrogen. The specimens were prepared by compression molding at $T = T_g + 50$ and 2 MPa for 15 min.

The measurements in the DMTA and RMS were carried out at the same frequency, γ = 1 Hz, and the same heating/cooling rate of 2 °C/min. Frequency scans at γ from 0.016 to 16 Hz were conducted for PIP–Cu-1.0 between 308 and 358 K in order to verify the time–temperature superposition at $T > T_g$.

Results

Figure 1 illustrates the dependence of the storage (E') and the loss (E'') tensile moduli at γ = 1 Hz for the PIP–Cu. Representative data are listed in Table II. In the

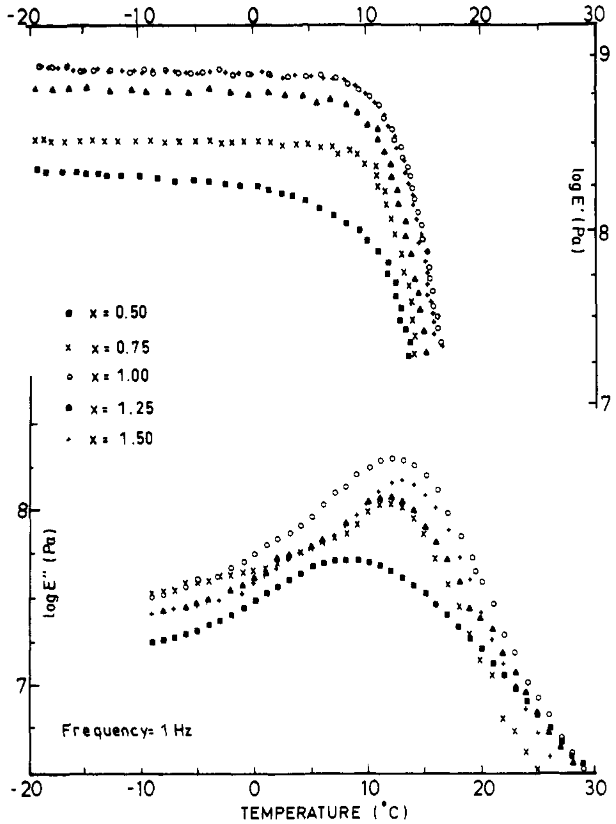

Figure 1. Storage and loss moduli vs temperature in the glassy state for PIP(NMe_2)$_2$-5K complexed with $CuCl_2$.

glassy state, when x changes from 0.50 to 1.0, E' increases regularly from 200 MPa to 1 GPa (Figure 1). E' does not increase any more when the Cu to amine molar ratio increases further to $x = 1.5$. Surprisingly enough, a smaller value is reported for the intermediate ratio of 1.25. Whatever the property investigated in this study, that anomaly is repeatedly observed. The E'' peak position values of the glass-to-rubber transition (T_{gi}), read from Figure 1, are listed in Table II. It is evident that, similar to the DSC-based glass transition temperature, T_g (Table II), the T_{gi} is also independent of the metal to amine ratio, x, within the experimental error.

Figures 2 and 3 show the thermal dependence of the isochronous torsion modulus of α,ω-dipiperazinopolybutadiene complexed with various amounts of $CuCl_2$ and $FeCl_3$. The main parameters of these curves are listed in Table III. Before addition of the transition-metal salts, the PBD sample was a viscous liquid, unsuitable for torsion modulus measurements. By contrast, a rubberlike behavior is clearly observed in the Cu- and Fe-complexed telechelic polymer.

For the metal to amine ratio $x = 1$, a well-defined rubbery plateau is observed. Values of the inflection temperature, T_{gi} (at the halfway point from the glassy to the rubbery plateau), of the mid rubbery plateau modulus and of the mid rubbery plateau temperature (T_e) are shown in Table III. It is evident that for PBD–Cu-1 and PBD–Fe-1 these values are similar. However, the onset of the viscous flow for the former polymer occurs at the temperature 20 °C higher than the latter.

The data in Figures 2 and 3 show a large difference in the viscoelastic behavior of the PBD–Cu and the PBD–Fe samples when the metal to amine ratio is different from 1. For PBD–Cu, with $x = 0.5$–3 (Figure 2), all the data are confined to a rather narrow envelope, with the rubbery plateau modulus changing by a factor of 1.8. On the other hand, for PBD–Fe with the same range of the molar ratio x, the plateau modulus changes by more than 1 decade. When $x = 0.5$, the rubbery plateau region of both samples is reduced in both size and magnitude. The data on creep, stress–strain, and stress relaxation showed a similar behavior.[22]

Complexation of the piperazine end groups with an excess of $FeCl_3$ results in a significant increase of the rubbery plateau modulus (Figure 3), but its width does not change. Apparently, Fe^{3+} generates a more rigid transitional network than Cu^{2+} does, but in both systems the complexes disintegrate at a similar temperature.

As reported in Table II, complexation of the dimethylamine end groups of PIP by $CuCl_2$ is responsible for an increase in T_g larger than that observed for α,ω-dipiperazinopolybutadiene. A common feature of these two telechelic polymers is that T_g does not depend significantly on the metal to amine ratio.

The storage (G') and loss (G'') shear moduli vs temperature curves for all the samples listed in Table I are presented in Figure 4. It is useful to define ΔT_R as a range of temperatures in the rubbery plateau zone in which $G' > G''$. The values of ΔT_R are also listed in Table II and give comparative information on the stability range of the rubber elasticity.

It is evident that PIP–Cu with the molar ratio $x = 0.5$ does not have distinct elastomeric character. Not only is ΔT_R small but also the viscoelastic functions do not show a rubbery plateau. As x increases above 0.5 there is a systematic change in the viscoelastic response; the rubbery plateau becomes more and more distinct and the relaxation associated with the network disintegration becomes sharper.[21]

It may be interesting to note that, as with the glassy modulus, E' (Figure 1), ΔT_R when plotted vs x shows a local minimum at $x = 1.25$. This means that structural features associated with the x ratio influence both the glassy and the rubbery regions.

Complexation of PIP(NR_2)$_2$ with Fe^{3+} also results in an elastic product (Figure 5). However, PIP–Fe-1 hardly resembles PIP–Cu-1. As a matter of fact G' of PIP–Cu-1.5 superimposes on that of PIP–Fe-1 in the full range of temperature (while G'' only superimposes at $T > 59$ °C). This observation is consistent with E' values in the glassy state.

Discussion

Glassy State. As shown in Figure 1 the value of the storage modulus E' depends on the copper to dimethylamine molar ratio, x. The values of E_G listed in Table II have been taken at an arbitrary constant value of $T_G = 0.939T_g$ (DSC) and are plotted vs x in Figure 6. It is evident that the modulus increases with the amount of $CuCl_2$ to reach a maximum value at $x = 1.0$. This means that the intermolecular association of the PIP(NR_2)$_2$ chains is the strongest at this peculiar ratio. The rigidity of the glassy material can thus be adjusted by varying the amount of $CuCl_2$ compared to the amine end groups. An excess of the salt does not necessarily reinforce the association of the end groups. For $x = 1.25$, Figure 6 shows what might be a disturbing action on the association of the amine end groups. However, for $x = 1.5$, the value of E' observed for the stoichiometric composition ($x = 1$) is regained. As discussed in a subsequent section, the irregular evolution of the storage modulus when x varies from 1.0 to 1.5 is also observed for the solution viscosity of samples prepared independently.

It is worth noting that the rigidity of the glassy PIP material is independent of whether copper(II) or iron(III) chloride has been used at a metal to amine molar

Table II
$PIP(NR_2)_2$-5K

sample	T_g,[a] K	ΔT_g,[b] K	ΔT_R,[c] K	T_{gi},[d] K	T_d,[e] K	E_G,[f] MPa	G_R,[g] kPa	T_m,[h] K	G_m,[i] kPa	n[j]
PIP–Cu-0.5	291	17	24	282		204	110			1.0
PIP–Cu-0.75	294	20	41	285		302	148			1.4
PIP–Cu-1.0	291	17	42	285	333	708	427	325	355	3.6
PIP–Cu-1.25	295	21	23	286	326	550	447	324	479	4.2
PIP–Cu-1.5	294	20	32	285	337	692	832	326	724	7.1
PIP–Fe-1.0	291	17	24		321	708	550	318	617	5.4

[a] For uncomplexed PIP, $T_g = 274$ K. [b] $\Delta T_g = T_g - 274$. [c] ΔT_R = range of temperature in the rubbery plateau zone where $G' > G''$. [d] $T_{gi} = T$ at the maximum of E'' in the glassy region. [e] $T_d = T$ at the maximum of G'' in the rubbery plateau. [f] $E_G = E'$ at $T = T_G = 0.939T_g$. [g] $G_R = G'$ at $T = T_R = 1.10T_g$. [h] $T_m = T$ at the minimum of G'' in the rubbery plateau. [i] $G_m = G'$ at $T = T_m$. [j] n = number of end groups per cross-link.

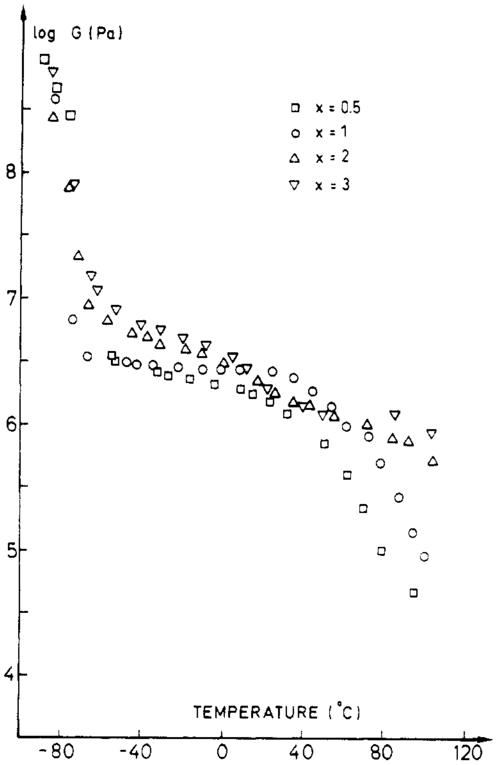

Figure 2. Isochronous modulus vs temperature for $PBD(pip)_2$-4K complexed with $CuCl_2$.

ratio of 1. Then the tensile storage modulus is maximum (708 MPa) and 15% higher than the value reported for the same $PIP(NR_2)_2$ quaternized with n-alkyl iodides.[21] In that series of experiments the maximum value of E' (617 MPa) was recorded for the methyl iodide quaternized $PIP(NR_2)_2$. On the other hand, when 1.5-diiodopentane was used as the quaternizing agent, E' = 1.02 GPa was obtained, i.e., 44% higher than the value observed for the complexed telechelic polyisoprene. It is thus obvious that both the complexation and the quaternization of the amino end groups lead to a significant stiffening of the polyisoprene matrix. The effect is quite spectacular considering the relatively small amount of the additives required (most often less than 5 mol %; Table I).

Transition Zone. Characterization of the PIP samples by DMTA (Figure 1), as well as that of PBD by torsion pendulum (Figures 2 and 3), is of interest. For PIP the values of T_{gi} corresponding to the peak position of G'' in the glassy region are listed in Table II while those for PBD are reported in Table III. T_{gi} has been considered as the temperature at the halfway point from the glassy to the rubbery plateau. Since the glassy plateau was not accessible using the Gehman torsion pendulum, T_{gi} values in Table III are only indicative.

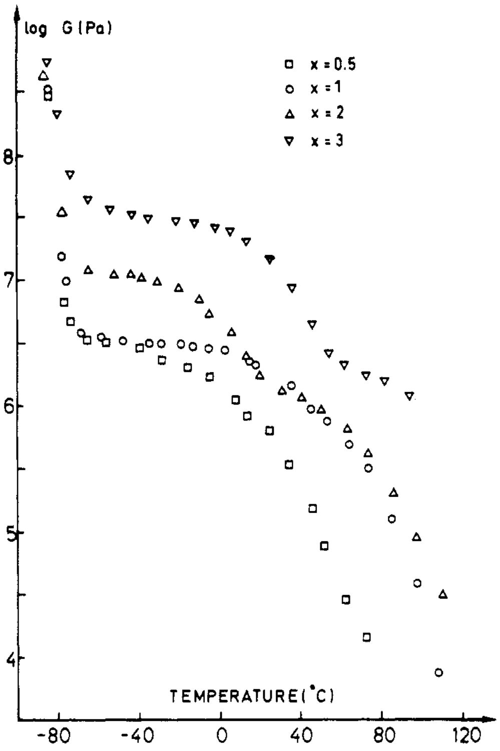

Figure 3. Isochronous modulus vs temperature for $PBD(pip)_2$-4K complexes with $FeCl_3$.

Table III
$PBD(pip)_2$-4K

sample	T_g,[a] K	ΔT_g,[b] K	T_{gi},[c] K	T_e,[d] K	G_e,[e] kPa	n[f]
PBD–Cu-0.5	202	5	(199)	(263)	220	(1.8)
PBD–Cu-1.0	199	2	(199)	263	290	2.4
PBD–Cu-2.0	205	8	(199)	(263)	365	(3.0)
PBD–Cu-3.0	207	10	(199)	(263)	429	(3.5)
PBD–Fe-0.5	199	2	(196)	(235)	284	(2.6)
PBD–Fe-1.0	201	4	(196)	251	318	2.7
PBD–Fe-2.0	201	4	(196)	233	1078	9.9
PBD–Fe-3.0	202	5	(196)	264	2773	22.5

[a] For uncomplexed PBD, $T_g = 197$ K. [b] $\Delta T_g = T_g - 197$. [c] $T_{gi} = T$ at the halfway point from the glassy to the rubbery plateau. Since the glassy plateau was not experimentally accessible, T_{gi} values are only indicative and reported in parentheses. [d] T_e = mid rubbery plateau temperature. [e] $G_e = G$ at $T = T_e$ ($E_e = 3G_e$ for an ideal rubber; i.e., Poisson ratio = 0.5). [f] n = number of end groups per cross-link.

The glass transition temperature (by DSC) of $PIP(NR_2)_2$ ($\bar{M}_n = 5200$) is 274 K. For the alkyl iodide quaternized material, T_g decreases with increasing length of the alkyl chain from 311 to 265 K.[21] For the complexed $PIP(NR_2)_2$, both T_g and T_{gi} show slight variation with the metal to amine molar ratio x, especially for $x > {}^1/_2$. Considering the experimental error, the average values for PIP–Cu ($T_{gi} = 285 \pm 2$ K and $T_g = 293 \pm 2$ K) and for PBD (T_{gi} = 198 ± 2 K and $T_g = 202 \pm 3$ K) seem to be reasonably

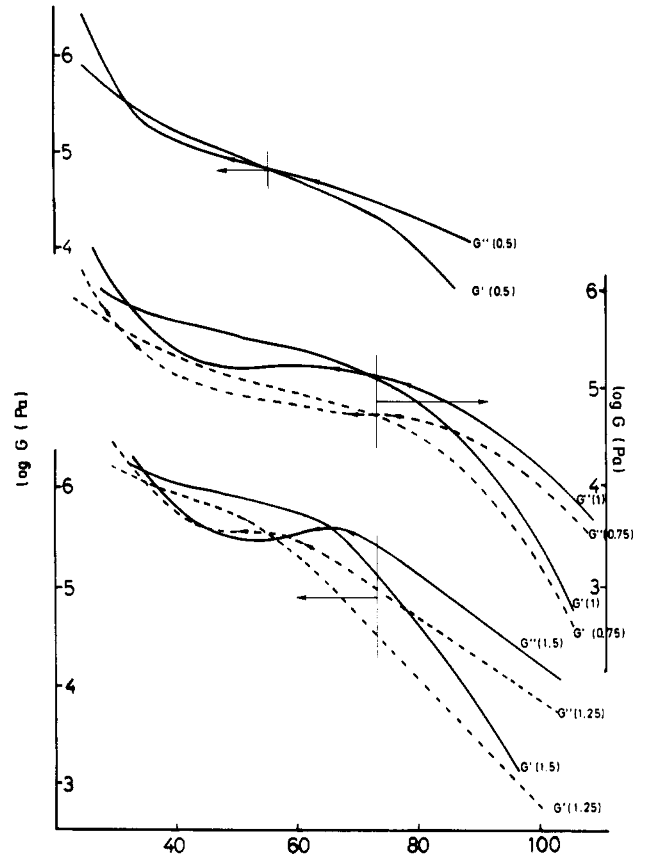

Figure 4. Shear moduli vs temperature for PIP(NMe$_2$)$_2$-5K-Cu: x = 0.5, 0.75, 1.0, 1.25, and 1.5, respectively.

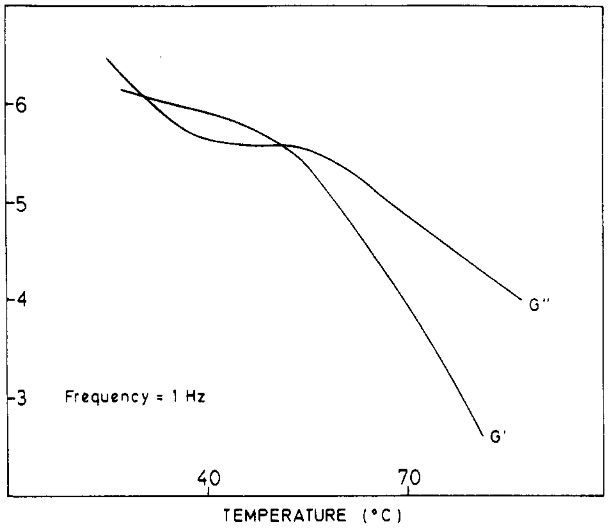

Figure 5. Shear moduli vs temperature for PIP(NMe$_2$)$_2$-5K-Fe-1.0.

constant. It is worth noting that both T_{gi} and T_g for complexed PIP(NR$_2$)$_2$ are comparable to values reported for the methyl iodide quaternized sample;[21] viz., T_{gi} = 296 K and T_g = 311 K.

ΔT_g, i.e., the change in T_g due to the complexation (or the quaternization) of the amino end groups of PIP, is also shown in Tables II and III. For PBD, ΔT_g is 5 ± 3 °C while for PIP, its value is 19 ± 2 °C. These values have to be compared to ΔT_g, which is found in the range from +37 to -9 °C for the quaternized PIP(NR$_2$)$_2$.[21]

Rubbery Plateau. Let us consider first the piperazine-terminated PBD. It is generally accepted that the Cu^{2+} and Fe^{3+} cations are able to coordinate at least four amino groups.[23] That particular situation corresponds to a metal to piperazine end-group molar ratio of 0.5 as illustrated by Chart I. Although the "chair" conformation is usually assigned to piperazine, one can expect that this diamino group acts as a chelate for the transition-metal ions. In that respect, a solid complex of Pd with N,N'-dimethylpiperazine in the "boat" conformation has been reported elsewhere.[24] Moreover, a thermodynamic study has shown that piperazine and closely related compounds coordinated Cu(II) ion as bidentate ligands.[25] A chain-extension process should therefore occur with formation of longer linear and/or cyclic macromolecules. This modification can enhance chain entanglements and chain entrapments into catenanes. Thus a rubbery behavior can be generated as observed in Figures 2 and 3. In the time scale of the measurements (10 s), the thermal stability of the related chain network is poor as shown by the slow but regular decrease of the modulus in the rubbery region upon increasing temperature. This is in agreement with the ill-defined structure of the chain network, i.e., a mixture of linear and cyclic chains stabilized by coordinative bonds.

The coordination of one piperazine end group to one metal cation (x = 1.0) is illustrated by Chart II. In this case, each end group is more likely to coordinate a metal cation and associate into dimers by coordinative and/or dipole–dipole interactions. This should lead to a network formation as reflected by the rubberlike plateau observed in Figures 2 and 3. The driving force for the end groups to associate would be more coordinative than ionic. Let us mention that the association of the ion pairs in ionomers may be viewed as a complexation process due to the trend of a metal cation to be coordinatively

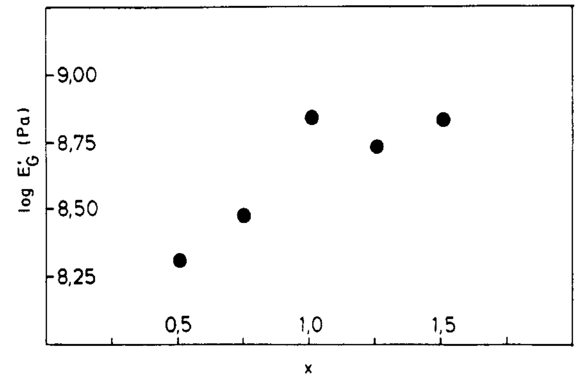

Figure 6. Storage modulus vs Cu/amine ratio (x) in the glassy state for PIP(NMe$_2$)$_2$-5K complexed with CuCl$_2$ (frequency = 1 Hz, T = 0.939Tg (DSC)).

Chart I

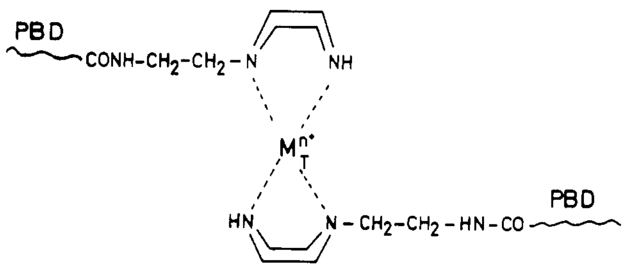

Chart II

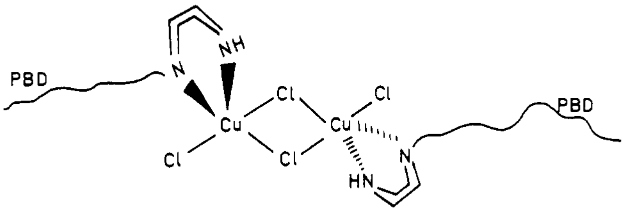

surrounded with one or several electron donors (anions, ligands).[26] Clearly, the amino telechelic polybutadienes coordinated to copper or iron chlorides are insoluble in both polar and nonpolar solvents (heptane, toluene, $CHCl_3$, THF, toluene/methanol mixtures, etc.). This supports the more coordinative than ionic character of the end groups association. The condition required for a network formation is that at least two end groups associate. It means that two metal chlorides have to be closely paired as dimers (Chart II). Such a structure has already been observed by X-ray scattering for similar dichloro(*N*,*N*,*N*′,*N*′-tetramethylethylenediamine)copper(II) complexes).[27]

The thermal stability of the "coordinative" aggregates results from both the thermodynamics (metal–ligand complexation constants) and the kinetics of the complexation process.[26] Little information is available for copper and iron amino complexes in low dielectric constant media. It is however known that, in polar solvents such as water or alcohols, copper(II) is the most efficient transition metal in stabilizing amino complexes.[23] This trend has been supported by the thermomechanical behavior of a butadiene–styrene–4-vinylpyridine copolymer coordinated to transition-metal salts.[16]

As shown in Table III the values of the plateau modulus, G_e, increase with x. G_e is defined as the isochronous modulus at T_e, where T_e is the mid rubbery plateau temperature (see Figures 2 and 3). The increase in the Cu^{2+} series is less dramatic than that in the Fe^{3+} series.

According to the Rouse theory of the rubber elasticity, the plateau modulus is a function of the molecular weight between cross-links, M_c. For the studied systems, M_c can be approximated to $\bar{M}_n$ of the polydiene, and the number of amino end groups per cross-link can be written as[29]

$$n = 4\bar{M}_n G_e / \rho_e R T_e \qquad (1)$$

where ρ_e is the polymer density at T_e and R is the gas constant. $\rho_e T_e$ can be approximated to a constant, and, accordingly, n is proportional to G_e in the limit of validity of eq 1. For PIP–Cu, n values have been calculated (see Table II) from G_R and G_m, where G_R is defined as a value of G' at $T_R = 1.10T_g$ and G_m as G' at the minimum value of the G'' vs T curve. Values of n reported in Tables II and III have been plotted vs x on Figure 7. For the x values considered in this study, a power law dependence is observed:

$$n = Kx^{\alpha} \qquad (2)$$

The least-squares fits of the experimental data give the following values for the parameters α and K ($K = n$, when $x = 1$):

PBD–Fe	$\alpha = 1.92$	$K = 2.67$	$r^2 = 1.0$
PBD–Cu	$\alpha = 0.366$	$K = 2.35$	$r^2 = 0.997$
PIP–Cu	$\alpha = 1.82$	$K = 3.10$	$r^2 = 0.95$

r^2 is the least-squares linear regression coefficient. The plots are presented in Figure 7.

By definition

$$x = n_M / n \qquad (3)$$

where n_M is the number of metal cations per cross-link. Therefore, eq 2 can be rewritten as follows:

$$n^{1+\alpha} = K n_M \qquad (4)$$

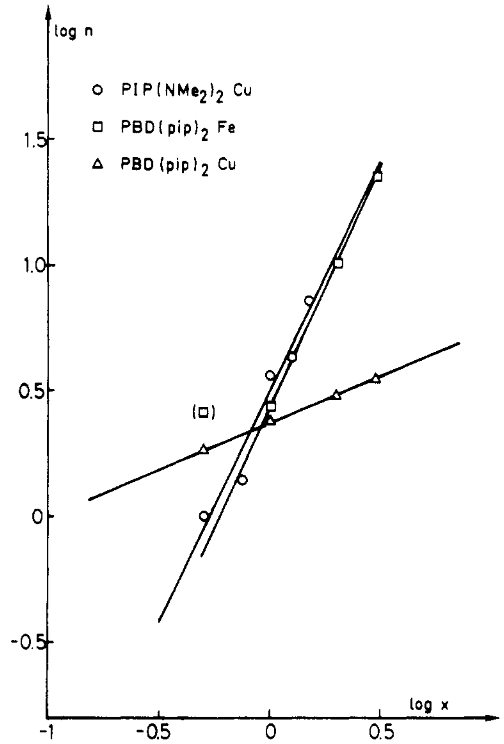

Figure 7. Logarithmic plot of number of end groups per cross-link (n) vs metal/end group ratio (x) for the complexed polydienes.

For $\alpha = 2$ (PBD–Fe and PIP–Cu), eq 4 becomes

$$n = K^{1/3} n_M^{\,2/3} \qquad (5)$$

If the number of piperazine end groups (n) per cross-link is, roughly, proportional to the aggregate surface and if we consider that the volume of an aggregate surface and if we consider that the volume of an aggregate is proportional to the metal amount (n_M), eq 5 seems to be a reasonable approximation since the surface has to be proportional to its volume at the power $^2/_3$. Therefore, a three-dimensional growth could be postulated for the PBD–Fe and the PIP–Cu series. On the other hand, for the PBD–Cu, n increases much slower with x ($\alpha = {}^1/_3$), supporting that a three-dimensional growth does not occur. In both PBD and PIP systems with Cu^{2+} at $x = 1$, infinitely long linear chains are expected to be formed. Interestingly, for poly(4-vinylpyridine) coordinated with Cu^{2+} at $x = 1$, Agnew reported dimerization.[34] Thus, n values slightly higher than 2 (for $x = 1$) may originate from both entanglement and ion pairing as already discussed for an α,ω-dicarboxypolyisoprene of $\bar{M}_n = 8000$ neutralized with various metal cations.[30] The most puzzling observation is the rate at which n increases with x, when x is greater than 1. If α,ω-dipiperazinopolybutadiene does not lead to a three-dimensional structure with $CuCl_2$, then why does α,ω-bis(dimethylamino)polyisoprene lead to a rapidly extended complexation? One possible explanation may be that the amide function of the piperazine end group of PBD contributes to the partial intramolecular coordination of Cu^{2+} ions. Another explanation could be the chelating behavior of the piperazine unit in contrast to the dimethylamino end group. The piperazine ligand needs two coordination sites on the Cu^{2+} cation to act as a chelate whereas only one site is required for the complexation of the dimethylamine unit. As a result of their less hindered structure, the dimethylamine end groups should be coordinated more extensively to the linear chains of $CuCl_2$ (Chart III)[31-33] than the piperazine

Chart III

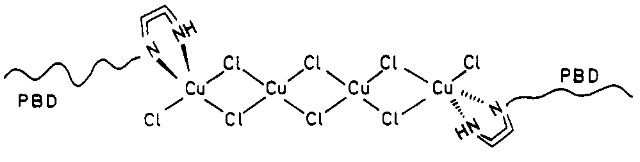

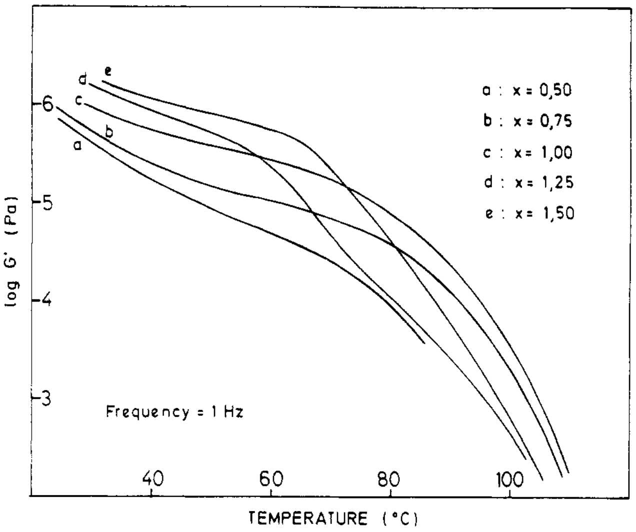

Figure 8. Storage shear modulus vs temperature in the rubbery state for $PIP(NMe_2)_2$-5K–Cu.

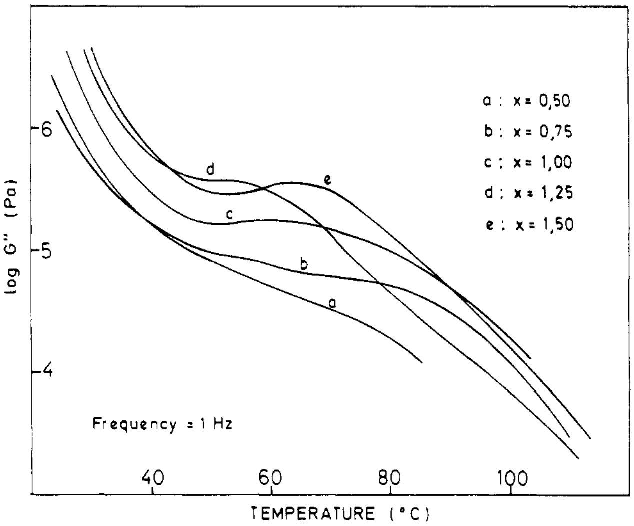

Figure 9. Loss shear modulus vs temperature in the rubbery state for $PIP(NMe_2)_2$-5K–Cu.

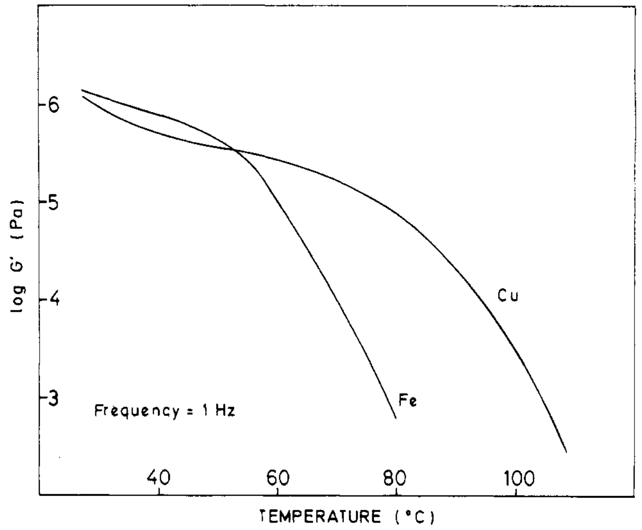

Figure 10. Storage shear modulus vs temperature in the rubbery state for $PIP(NMe_2)_2$-5K complexed with $CuCl_2$ and $FeCl_3$, respectively (x = 1.0).

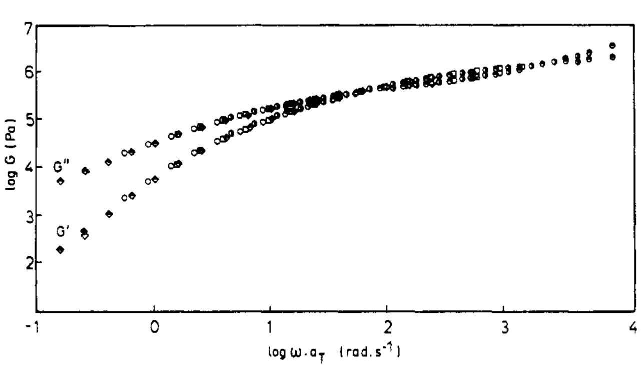

Figure 11. Shear moduli vs reduced frequency for $PIP(NMe_2)_2$-5K-Cu-1.0. Reference temperature: (◒) 35 °C, (◑) 40 °C, (□) 45 °C, (○) 50 °C, (◇) 55 °C, (◆) 60 °C.

groups. This situation does not hold for $FeCl_3$, since it forms three-dimensional structures rather than linear ones.

Terminal Zone. The data from the RMS scan of the PIP–Cu samples are replotted in Figures 8 and 9, respectively, as G' and G'' vs T. The data in the latter figure indicate a gradual increase with x of the secondary relaxation peak at T_d ($>T_g$). As shown in Table II, T_d varies with x in a nonmonotonic fashion. Since T_d limits the range of the rubbery properties, it may be considered as the dissociation temperature of the end-group aggregates. This means that, in the time scale of the experiments, the association equilibrium of the end groups at T_d is in favor of the unassociated species and allows flow to occur. At $T > T_d$, the complexed $PIP(NR_2)_2$ shows a viscoelastic flow behavior. As the sharpness of the G'' peak indicates a narrow distribution of the relaxation times, it is evident that the polymer structure becomes stiffer but not necessarily more stable when x increases from 1 to 1.25. Only at x = 1.5 are both stable stiffening and a narrow range of relaxations (dicompositions) obtained.

It is worth recalling that α,ω-bis(dimethylamino)polyisoprene complexed with various amounts of $CuCl_2$ is soluble in a range of low polarity solvents, such as toluene, THF, and toluene/methanol (98/2, v/v) mixture. The concentration dependence of the specific viscosity in toluene at 25 °C has been investigated using a complexed $PIP(NR_2)_2$ sample of 18 000 $\bar{M}_n$.[28] As a rule the relative position of the experimental curves in the specific viscosity scale depends on the metal to amine molar ratio. The viscosity increases when x goes up from 0.33 to 1.0. Then it decreases as x increases from 1.0 to 1.25, and finally it increases again at x higher than 1.25. It means that the solution viscosimetric behavior parallels the viscoelastic behavior in terms of the dependence on x, although these data have been reported for two series of polymers prepared in an independent way.

From the comparative data in Figure 10, it is evident that at x = 1 PIP–Fe is much less stable than PIP–Cu. Note that T_d (Table II) for the latter polymer is higher by 12 °C and the G' decrease with T is more gradual than that for the former.

For PIP–Cu with x = 1, the frequency sweeps were obtained at T = 308–358 K. The master curve was constructed by the horizontal shifting of isotherms onto one at the reference temperature, T_R = 333 K. As shown in Figure 11, a good superposition in the terminal and rubbery plateau zones is obtained for both G' and G''. At

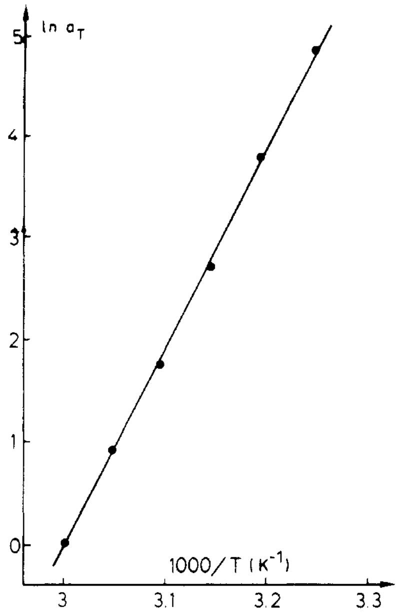

Figure 12. Plot of shift factors vs $1/T$ for PIP(NMe$_2$)$_2$-5K-Cu-1.0.

low temperatures ($T < T_R$) the horizontal shift factors, a_T, follow an Arrhenius relation fairly well, giving the activation energy of flow: $\Delta H_a = 165$ kJ/mol (Figure 12). This value is the highest activation energy obtained so far for the relaxation of mutually interacting groups selectively attached at the ends of short length polydienes, i.e., metal carboxylates[20,29] and quaternary ammoniums.[21] This increase in ΔH_a is in contrast to the decrease of T_i and the equilibrium modulus of the rubberlike plateau. An activation energy of 117 kJ/mol was determined for a poly(butadiene-*co*-styrene-*co*-4-vinylpyridine) cross-linked by $NiCl_2 \cdot 2H_2O$ (the number of nickel ions per pyridine side group was 1.23). The authors attributed that relaxation to clusters of complexes, the exchange of which broke and re-formed the cross-links.[16]

Conclusions

Upon the complexation of the amino end groups of low molecular weight polydienes, a rubberlike plateau emerges, which is absent in the original polymers.

The molar ratio, x, of the transition-metal salt to the polymer end group strongly affects the linear viscoelastic behavior. With an increase of x the value of the modulus in the glassy state increases, and so do the width of the rubbery plateau and the temperature, T_d, at which the flow takes place. The optimum properties are obtained at $x = 1$. Although the level of complexation is higher for Fe^{3+} than for Cu^{2+}, the stability of the complex is higher for the latter metal ions.

When the complex formed by the α,ω-dipiperazinopolybutadiene with Cu^{2+} is compared to that of α,ω-bis(dimethylamino)polyisoprene, the viscoelastic properties at $x = 1$ seem comparable. However, upon addition of a further amount of Cu^{2+}, the rate of increase of the rubbery plateau modulus of the former is about 6 times slower than that of the latter.

Thus, both quaternizaton[21] and complexation of α,ω-diamino polydienes are efficient means of improving the viscoelastic properties of the polymer. Adjusting the paraffinic chain length of the quaternizing agent or the molar ratio of the metal salt to amine end group allows for selection of the desired behavior. The thermoreversible associations of the chain extremities could help initially immiscible polymers to get intimately mixed. The application of that concept has already been reported for telechelic polymers,[35-37] and it will be extended in a forthcoming paper.

Acknowledgment. P.C., R.J., and Ph.T. are grateful to the "Services de la Programmation de la Politique Scientifique" (Brussels) for financial support. P.C. thanks the "Institut pour l'encouragement de la recherche scientifique dans l'industrie et l'agriculture" (IRSIA) for a fellowship and the "Fonds National de la Recherche Scientifique" (FNRS) for having awarded him a grant to visit the Industrial Materials Research Institute (IMRI) of Montreal. He is very much indebted to IMRI for the opportunity of spending a 3-mo stay in their facilities. The skillful technical assistance of P. Sammut (IMRI) for dynamic mechanical measurements is very much appreciated and so is the contribution of J. P. Hautekeer (University of Liège) for the torsion pendulum measurements.

References and Notes

(1) Eisenberg, A.; King, M. *Ion Containing Polymers*; Academic Press: New York, 1977.
(2) MacKnight, W. J.; Earnest, T. R., Jr. *J. Polym. Sci., Macromol. Rev.* **1981**, *16*, 41.
(3) Kaneko, M.; Tsuchida, E. *J. Polym. Sci., Macromol. Rev.* **1981**, *16*, 397.
(4) Pomogailo, A. D.; Savostyanov, V. S. *J. Macromol. Sci., Rev. Macromol. Chem. Phys.* **1985**, *C25* (3), 375.
(5) Foxman, B. M.; Gersten, S. W. *Encyclopedia of Polymer Science and Engineering*; Wiley: New York, 1985; Vol. 4, p 175.
(6) Teyssié, Ph.; Decoene, C.; Teyssié, M. T. *Makromol. Chem.* **1965**, *84*, 51.
(7) Lekchiri, A.; Morcellet, J.; Morcellet, M. *Macromolecules* **1987**, *20*, 49.
(8) Barbucci, R.; Casolaro, M.; Corezzi, S.; Reginato, G. *Polymer* **1986**, *27*, 1986.
(9) Kratz, M. R.; Hendricker, D. G. *Polymer* **1986**, *27*, 1641.
(10) Kobayashi, S.; Hiroishi, K.; Tokunoh, M.; Saegusa, T. *Macromolecules* **1987**, *20*, 1496.
(11) Pappalardo, S.; Bottino, F.; Finocchiaro, P.; Mamo, A. *J. Polym. Sci., Part A* **1987**, *25*, 1793.
(12) Nagai, A.; Takahashi, A.; Komatsu, T.; Nakawaga, T. *Polym. J.* **1988**, *20*, 609.
(13) Potts, K. T.; Usifer, D. A. *Macromolecules* **1988**, *21*, 1985.
(14) Sen, A.; Weiss, R. A. *Polym. Mater. Sci. Eng., Prepr.* **1988**, *58*, 981.
(15) Lundberg, R. D.; Phillips, R. R.; Peiffer, D. G. *J. Polym. Sci., Polym. Phys. Ed.* **1989**, *27*, 245.
(16) Meyer, C. T.; Pineri, M. *Polymer* **1976**, *17*, 382.
(17) Jérôme, R.; Broze, G. *Rubber Chem. Technol.* **1985**, *58*, 223.
(18) Jérôme, R. *Integration of Fundamental Polymer Science and Technology*; Kleintjens, L. A., Lemstra, P. J., Eds.; Elsevier: London, 1986; p 242.
(19) Jérôme, R. *Telechelic Polymers: synthesis and applications*; Goethals, E., Ed.; CRC Press: Boca Raton, FL, 1989; Chapter 11.
(20) Horrion, J.; Jérôme, R.; Teyssié, Ph.; Marco, C.; Williams, C. E. *Polymer* **1988**, *29*, 1203.
(21) Charlier, P.; Jérôme, R.; Teyssié, Ph.; Utracki, L. A., submitted for publication.
(22) Tant, M. R.; Song, J. H.; Charlier, P.; Wilkes, G. L.; Jérôme, R., to be published.
(23) Ashcroft, S. J.; Mortimer, C. T. *Thermochemistry of Transition Metal Complexes*; Academic Press: London and New York, 1970.
(24) Hassel, O.; Perdersen, B. F. *Proc. Chem. Soc.* **1959**, 394.
(25) Pagano, J. M.; Goldberg, D. E.; Fernelius, W. C. *J. Phys. Chem.* **1961**, *65*, 1062.
(26) Minoux, J. *Inf. Chim.* **1974**, *130*, 191.
(27) Estes, E. D.; Estes, W. E.; Hatfield, W. E.; Hodgson, D. J. *Inorg. Chem.* **1975**, *14*, 106.
(28) Charlier, P.; Jérôme, R.; Teyssié, Ph., accepted for publication in *Macromolecules*.
(29) Broze, G.; Jérôme, R.; Teyssié, Ph.; Marco, C. *J. Polym. Sci., Polym. Phys. Ed.* **1983**, *21*, 2205.
(30) Register, R. A.; Foucart, M.; Jérôme, R.; Ding, Y. S.; Cooper, S. L. *Macromolecules* **1988**, *21*, 1009.

(31) Rundle, R. E. *J. Am. Chem. Soc.* **1957**, *79*, 3372.
(32) Engberg, A. *Acta Chem. Scand.* **1970**, *24*, 3510.
(33) Wertz, D. L.; Tyvoll, J. L. *J. Inorg. Nucl. Chem.* **1974**, *36*, 3713.
(34) Agnew, N. H. *J. Polym. Sci., Polym. Chem. Ed.* **1976**, *14*, 2819.
(35) Russell, T. P.; Jérôme, R.; Charlier, P.; Foucart, M. *Macromolecules* **1988**, *21*, 1709.
(36) Sen, A.; Weiss, R. A. *Polym. Mater. Sci. Eng.* **1988**, *58*, 981.
(37) Peiffer, D. G.; Duvdevani, I.; Agarwal, P. K.; Lundberg, R. *J. Polym. Sci., Polym. Lett.* **1986**, *24*, 581.

Theory of Adsorbed Block Copolymers

M. D. Whitmore*

Department of Physics, Memorial University of Newfoundland,
St. John's, Newfoundland, Canada, A1B 3X7

J. Noolandi*

Xerox Research Centre of Canada, 2660 Speakman Drive,
Mississauga, Ontario, Canada, L5K 2L1

Received September 19, 1989

ABSTRACT: We present a study of adsorbed diblock copolymers, which is based on the mean-field self-consistent theory of incompressible polymer/solvent blends. We assume that one of the blocks is tightly adsorbed and model the remaining block using the formalism recently developed for crystallizable/amorphous block copolymer blends. Restricting attention primarily to near-Θ conditions, we present series of calculations describing adsorption at a single surface and adsorption on two parallel surfaces a finite distance apart. For the second case, we calculate the long-range forces acting on the two surfaces. We make quantitative comparisons with experiment for conditions corresponding to slightly good, Θ, and slightly poor solvents. We determine the thickness and shape of the polymer density profiles, obtain approximate scaling relations and the ranges of their applicability, study finite molecular weight effects, as well as the extent of the interdigitation of layers adsorbed on opposite surfaces, and show how these quantities vary as the surface separation changes. In addition, we show how the scaling of the *apparent* range of the measured long-range force can differ from the scaling of the thickness of a single adsorbed layer.

1. Introduction

Polymer adsorption, in particular, homopolymer adsorption, has been extensively studied both experimentally and theoretically. In this paper we study adsorbed block copolymers and the resulting long-range forces acting on two surfaces with adsorbed copolymers. (We do not refer to the extensive literature on adsorbed *homo*polymers in this paper.)

The system is illustrated schematically in Figure 1. One or two surfaces are immersed in solution containing copolymers, which then adsorb. We assume that one block of the copolymer adsorbs tightly but that the second block has no particular surface affinity and extends to at least some degree into the solution. It is the nonadsorbed blocks that are of primary interest here. In fact, in this paper we assume that the only significant roles of the tightly adsorbed blocks are anchoring the dangling block and partially controlling the total surface coverage. The system is thus equivalent to a collection of grafted polymers and is frequently referred to as the polymer brush.

These systems have been studied experimentally by small-angle neutron scattering,[1,2] hydrodynamic thickness measurements,[3] and Israelachvili surface forces techniques.[4-9] The experiments provide information on the shapes and sizes of the density profiles and how they vary with, for example, molecular weight and solvent quality. Here we summarize very briefly some of the scaling results that were extracted, with a view to illustrating the range of results which we attempt to explain in this paper.

The SANS measurements, which provide a detailed picture of the density profile, were made on low molecular weight PEO-*b*-PPO-*b*-PEO copolymers adsorbed on particles.[1,2] The brush thickness was found to scale approximately as $Z_{\mathrm{PEO}}^{0.5}$, where Z_{PEO} is the degree of polymerization of the PEO blocks. Killmann et al. measured the hydrodynamic thickness of a PEO-*b*-PPO-*b*-PEO coated latex[3] and found a similar result: it scaled as $Z_{\mathrm{PEO}}^{0.55}$. Surface force experiments measure the long-range force on two crossed cylinders resulting from the interacting layers on each surface. Taunton et al.[5-7] used terminally adsorbed PS chains in toluene and xylene, with five degrees of polymerization ranging from about 250 to 6000. The range of the force scaled approximately as $Z^{0.6}$ (except for the highest molecular weight case). Hadziioannou et al. used[4] PV2P-*b*-PS, in which the PV2P adsorbs and the PS extends in solution. They interpreted their results in terms of the scaling theory[10-13] (described below) and concluded[14] that for the good solvent case the range of the forced scaled *linearly* with Z_{PS}. On the other hand, Ansarifar and Luckham[8] measured force curves for three sets of PV2P-*b*-PBS copolymers in toluene and found the onset of the force scaled as $Z_{\mathrm{PBS}}^{0.7}$. They also incorporated the data of Hadziioannou et al.[4] and concluded that both sets of measurements are consistent with this $Z^{0.7}$ dependence. Finally, Marra and Hair used high molecular weight PEO-*b*-PS copolymers.[9] When two particular cases were compared, $Z_{\mathrm{PS}} \simeq 850$ and $Z_{\mathrm{PS}} \simeq 2400$, the range of the force apparently scaled *faster* than linearly with Z_{PS}.

In order to qualitatively understand the full range of these results, it is useful to identify two limits, characterized in terms of the degree of polymerization of the dangling block Z_{A} and the average surface area per poly-

0024-9297/90/2223-3321$02.50/0